Sensors & Actuators: A. Physical 398 (2026) 117357

Contents lists available at ScienceDirect

Sensors and Actuators: A. Physical

journal homepage: www.journals.elsevier.com/sensors-and-actuators-a-physical

Electret gel interfaces of phthalo blue and plasticized PVC for enhanced vibrotactile actuation☆

Ganesh Shimoga [a,b,*], Eun-jae Shin [a], Seok-Han Lee [a], Mruthyunjayachari Chattanahalli Devendrachari [a], Dong-Soo Choi [c], Sang-Youn Kim [a,**]

[a] Interaction Laboratory, Future Convergence Engineering, Advanced Technology Research Center, Korea University of Technology and Education, Cheonan-si, Chungcheongnam-do 31253, Republic of Korea
[b] Department of Biotechnology and Nanomedicine, SINTEF Industry, Trondheim 7034, Norway
[c] Smart Interface and Extended Reality Laboratory, Department of Computer Engineering, Kumoh National Institute of Technology, Gumi 39177, Republic of Korea

ARTICLE INFO

Keywords:
Actuators
Copper (II) phthalocyanine
Exo-skin
Haptic interfaces
Polymer Nanocomposites
Polyvinylchloride
Virtual reality

ABSTRACT

High-*k* electret gels composed of copper (II) phthalocyanine nanoparticles (*np*CuPc) and plasticized polyvinyl chloride (*p*PVC) have been developed for the fabrication of smart, reliable vibrotactile actuator devices. These High-*k* electret gels were prepared by uniform distribution of *np*CuPc into *p*PVC in a stoichiometric ratio using a high-power ultrasonic probe, followed by a straightforward solution casting protocol. The interactions between *np*CuPc and *p*PVC in the hybrid high-*k* electret gel composites were analyzed in detail using various physicochemical characterization techniques. Additionally, these high-*k* electrets are used as dielectric interfaces for the fabrication of vibrotactile actuator devices, the *np*CuPc/*p*PVC hybrid composite electret gels demonstrated a low leakage current (~1.75 μA), indicating efficient electric power utilization during actuation. The *np*CuPc-*p*PVC-3 gel demonstrated an ultimate dielectric constant of ~343.0 at 1.0 Hz, which likely contributed to its excellent actuation performance and long-term durability. Moreover, the actuators made from *np*CuPc-*p*PVC-3 gels showed remarkable robustness, maintaining performance across three consecutive days of continuous use. Notably, its actuation performance remained highly stable, with only a slight decline from 0.88 g to 0.871 g, emphasizing its impressive reliability and endurance.

1. Introduction

The development of advanced haptic devices relies heavily on the fabrication of polymer composites with high dielectric constant (*k*) materials [1]. These materials enable efficient electromechanical transduction and enhanced electrostatic forces, which are essential for creating realistic tactile feedback in haptic devices. Recent advancements in nanostructured hybrid high-*k* dielectric materials and polymer composites have shown great promise for actuator applications [2]. These materials offer several advantages, including improved mechanical flexibility, which is essential for haptic devices that require repeated stretching and bending [3]. High-*k* materials and its hybrid polymer composites can be designed to have tunable dielectric properties, allowing for precise control over the electromechanical transduction process [4]. Furthermore, nanostructured hybrid high-*k* materials have been shown to have improved energy storage capabilities, which is significant for haptic devices that require rapid and precise actuation [5]. Notably, several high-*k* materials have been explored for haptic device applications. For instance, barium titanate (BaTiO3) has been utilized in various haptic device applications, including tactile

☆ Electronic supplementary information (ESI) available: Synthesis of unsubstituted bulk copper phthalocyanine (*b*CuPc), synthesis of copper phthalocyanine nanoparticles (*np*CuPc), MALDI-TOF mass spectra of as-prepared *b*CuPc, photographs of high-*k* electret *np*CuPc-*p*PVC gels, Table illustrating the influence of plasticizer concentration on gel texture, EDXA data for *np*CuPc and respective *np*CuPc-*p*PVC gels, histogram of particle size distribution for *np*CuPc-*p*PVC-3 gels obtained from triplicate DLS measurements, XPS graphs/analysis of *b*CuPc, *np*CuPC and *np*CuPc-*p*PVC gels, experimental design and environment for measurements of haptic performances of high-*k* electret *np*CuPc-*p*PVC gels, haptic performances of the *np*CuPc-*p*PVC gel-based soft vibrotactile actuators.

* Corresponding author at: Interaction Laboratory, Future Convergence Engineering, Advanced Technology Research Center, Korea University of Technology and Education, Cheonan-si, Chungcheongnam-do 31253, Republic of Korea.
** Corresponding author.
E-mail addresses: ganesh.shimoga@sintef.no (G. Shimoga), sykim@koreatech.ac.kr (S.-Y. Kim).

https://doi.org/10.1016/j.sna.2025.117357
Received 10 July 2025; Received in revised form 20 November 2025; Accepted 1 December 2025
Available online 2 December 2025
0924-4247/© 2026 The Authors. Published by Elsevier B.V. This is an open access article under the CC BY license (http://creativecommons.org/licenses/by/4.0/).

actuators and sensors [6], while lead zirconate titanate (PZT) has also been widely employed in haptic devices, such as piezoelectric actuators and sensors [7]. Moreover, researchers have also investigated nanostructured polymer composites, such as those containing carbon nanotubes or graphene, for haptic device applications [8,9]. Building on these advancements, researchers are now developing innovative tactile actuators with microstructural dielectric polymer layers, carefully tuning their mechanical and dielectric properties to optimize performance [10,11]. In recent years, tremendous progress has been encountered in the development of nanostructured hybrid high-*k* dielectric materials and projecting their applications from flexible electronics to electronic skins [12].

Inserting high-*k* dielectric nanoparticles into a polymer matrix is an effectual strategy to elevate the dielectric constant and subsequently diminish the dielectric loss of polymer-based materials. This composite approach can drastically alter the physicochemical properties of the polymer nanocomposites. The improved elastic modulus with tuned dielectric properties of electrostrictive polymer nanocomposites can be used favorably in promising next generation electronic applications and to design sensors/actuators [13–15]. Due to unique characteristics of low dielectric loss, mechanical properties, high electric breakdown field, and easy processability, the polymer-based high-*k* materials are advantageous in the fabrication of charge-storage device, smart electronic skins and microelectromechanical systems (MEMS) [16–18].

Copper phthalocyanine (CuPc) is predominantly studied as high dielectric constant organic semiconductor from past several decades due to its high dielectric constant, possibly from the delocalization of electrons within its conjugated supramolecular structure [19]. Several researchers are documented the insertion of CuPc and CuPc oligomers (CuPc-o) into preferred polymers to enhance the dielectric properties and mechanical stability. Considering the complexity, geometry and static polarizability tensors of copper (Cu) metal in CuPc, the authors Ramprasad et al., [20] and Shi et al., [21] presented a principal Density-functional theory (DFT) approach for the investigation of dielectric properties of CuPc. Based on this classical model, it was revealed that, along the plane of the CuPc molecule the dielectric constants in the range (10–20) are expected. However, along the direction perpendicular to the plane of the CuPc molecule, a broad range of dielectric constants (>3 to ∞) can be attained. The supramolecules CuPc and CuPc-o are inserted in various polymer matrices to develop superdieletric polymer composites and documented its physicochemical/mechanical properties for technological applications. Series of CuPc-o loaded cyanophenyl-substituted and sulfated poly(aryl ether ketone) were reported by Yang et al., [22], with improved mechanical and dielectric properties. Wang et al., [23], synthesized CuPc-o nanoparticles (~10–20 nm size) and inserted into polyurethane. The authors presented preliminary characterizations and provided an approach to fabricate electromechanical actuators/artificial muscles. High elastic polyurethane foam was developed by Fan et al., [24], by loading CuPc-o and suggesting it as a promising candidate for the conversion of natural mechanical energy into electrical energy. Recently, by adopting prepolymerization technique *in-situ* composite sheets of novel phthalonitrile end-capped polyarylene ether nitrile/CuPc were reported by Tong et al., [25]. The authors investigated the increased dielectric properties (~3.2–5.0) with additional physicochemical properties.

Previously, we reported plasticized polyvinyl chloride (PVC) based vibrotactile actuators by loading silicon dioxide nanoparticles and polyaniline-coated silicon dioxide nanoparticles as dielectric fillers [26,27]. Inspired by the promising preceding results, in the present investigation we curiously started this research by loading different stoichiometric quantity of CuPc nanoparticles (*np*CuPc) to plasticized PVC (*p*PVC) to fabricate nanocomposite gels (*np*CuPc-*p*PVC) and utilized as dielectric interface for the fabrication of highly reliable smart vibrotactile actuators. All the fabricated nanocomposites were physicochemically characterized using an advanced analytical equipment and actuation performances were investigated in detail. The optimized composition (*np*CuPc-*p*PVC-3) provides a balanced interface between the phthalocyanine nanoparticles and the plasticized PVC matrix, which enhances charge retention and mechanical compliance. This synergy results in improved electromechanical coupling and higher displacement under actuation conditions.

2. Material and methods

2.1. Chemicals used

Phthalonitrile, anisole, glycerol, trifluoroaceticacid (TFA), 1,8-diazabicyclo(5.4.0)undec-7-ene (DBU), are purchased from TCI chemicals, Tokyo, Japan and used without further purification. Polyvinylchloride (Mw ~233000), Copper(II) acetate hydrate, and acetyltributylcitrate (ATBC, ~98.0 %), were procured from Sigma Aldrich, Seoul, South Korea. All the other chemicals and solvents are of reagent grade and used as received. HPLC grade water was used throughout the study.

2.2. Fabrication of npCuPc doped plasticized PVC nanocomposite gels (npCuPc-pPVC)

The detailed synthesis procedures for both unsubstituted bulk copper phthalocyanine (*b*CuPc) and copper phthalocyanine nanoparticles (*np*CuPc) are provided in the Supplementary Information. The MALDI-TOF mass spectrum with *b*CuPc is displayed in Fig. S1. {MS (MALDI-TOF) *m/z*: calc.: 576.07; found: 574.02 $[M-H]^-$}.

Eco-friendly plasticizer, acetyltributylcitrate (ATBC) was used for PVC and the weight ratio of ATBC was carefully optimized and it was kept constant throughout the experiment. In brief, 1 g of PVC was dissolved in ~ 20 mL of tetrahydrofuran (THF) at room temperature (~ 22 °C), a known amount *np*CuPc was loaded and probe sonicated (VCX750, 750 Watt) for 30 min. To this well dispersed solution, 5 g of ATBC plasticizer was added followed by probe sonication for 30 min. Series of *np*CuPc loaded PVC solutions with variable amount of *np*CuPc was prepared and designated as *np*CuPc-*p*PVC-1, *np*CuPc-*p*PVC-3, *np*CuPc-*p*PVC-5, *np*CuPc-*p*PVC-7, and *np*CuPc-*p*PVC-9. (For the preparation of *np*CuPc-*p*PVC-3 nanocomposite gels, 1 g of PVC, 30 mg of *np*CuPc, and 5 g of ATBC were used). The nanocomposite solutions were cast on the glass dish and subsequently peeled off after 72 h. Furthermore, considering the Hooke's law of elasticity [28], since the displacement of the deformation is directly proportional to the distorting force, the wave-shaped *np*CuPc-*p*PVC gels were also fabricated with the purpose of maximizing the displacement in our thin designed actuators. The wave-shape *np*CuPc-*p*PVC gels were obtained by pouring respective nanocomposite solution into a carved Teflon dishes to obtain the wave-shaped nanocomposite gels with 0.4 mm of thickness (with precise distance between two ridges = 2 mm) was detached from the Teflon dish after 72 h. For comparison, *np*CuPc was also loaded to unplasticized PVC. (For photographs of flat and wave-shaped *np*CuPc-*p*PVC-3 gels, see Fig. S2. in supplementary information). PVC gel texture was assessed visually and by touch (firm, elastic, sticky), and stability was determined as the time before syneresis or plasticizer leakage occurred. Later, the optimized gels were subjected to physicochemical characterization to evaluate their structural and functional properties. Stability was assessed over a 30-day period, considering the time before syneresis or plasticizer leakage occurred. The optimization results for gel texture and stability (including plasticizer leakage) are summarized in Table S1.

3. Physicochemical and spectral characterization

3.1. Morphological, dynamic light scattering (DLS), and energy dispersive X-ray analysis (EDXA)

It is crucial to determine morphological features of the fabricated nanocomposite gels to find out the nanosized CuPc synthesis and its homogeneous distribution in the PVC matrices. The surface, cross-

sectional morphology and elemental mapping/composition of the fabricated *np*CuPc-*p*PVC gels were analyzed using Field Emission Scanning Electron Microscopy (FESEM) and Energy dispersive X-ray analysis (EDXA). The FESEM images of synthesized *np*CuPc was presented in Fig. 1(a-b). The surface and cross-sectional FESEM images of *np*CuPc-*p*PVC-3 gel was displayed in Fig. 1(c-d).

From the high resolution FESEM image (Fig. 1b) it is clear that, the prepared *np*CuPc are nanosized and are in the range < 50–60 nm. Due to self-assembling of *b*CuPc under the adopted reaction conditions, the hydrothermally synthesized *np*CuPc portrayed slightly deformed spherical structure into soft edged short rod textured nanostructures. (See in supplementary information, Fig. S3. for energy dispersive X-ray analysis of as-prepared *np*CuPc, demonstrating the atomic composition of *np*CuPc). The energy dispersive X-ray analysis of as-prepared *np*CuPc, demonstrates the elemental composition of *np*CuPc (C - 65.17 %, N - 20.69 %, and Cu – 14.14 %). The uniform distribution of *np*CuPc throughout the PVC matrices was confirmed by FESEM and EDXA (See Fig. S4 and Fig. S5. in supplementary information for the energy dispersive X-ray analysis of surface and cross-sectional images/ elemental mapping of *np*CuPc-*p*PVC-3 gels, respectively). It is clear from the Fig. 1(c). that, there is no agglomeration of *np*CuPc on the PVC surface was noticed and it was further confirmed by the cross-sectional FESEM image [Fig. 1(d).].

The particle size and size distribution of *np*CuPc-*p*PVC-3 gels in colloidal THF suspensions were quantitatively analyzed using Dynamic Light Scattering (DLS). This technique determines particle size by measuring Brownian motion and applying the Stokes–Einstein equation. Measurements were performed with a Zetasizer Nano ZS (Malvern Instruments, UK) at a fixed scattering angle of 173° under ambient conditions (Lab temperature ~ 22 °C). The measurements were done in triplicate, for each analysis, 100 mg of *np*CuPc-*p*PVC-3 gels were dissolved in 100 mL of THF, and measurements were repeated to ensure reproducibility. The resulting size distribution histograms (Fig. S6) indicate that particles are primarily in the range of 50–65 nm, with an overall distribution within. These findings are consistent with morphological observations from FESEM analysis.

3.2. Raman, X-ray diffraction (XRD), X-ray photoelectron spectroscopy (XPS) and thermogravimetric (TG) analysis

The structural features of PVC, ATBC, *np*CuPc and physicochemical interaction of *np*CuPc with *p*PVC were investigated using Raman and XRD measurements. The displayed Raman spectra in Fig. 2a. depicts an intense Raman band at 632 and 698 cm^{-1} for PVC (powder), which corresponds to the stretching vibrations of C-Cl bonds. The C-H stretching vibrations of PVC in -CH_2- segmental structure had appeared at 2913 cm^{-1}. Similar C-H stretching vibrations (2886 – 2990 cm^{-1}) were also observed for ATBC [29]. Due to plasticization, the *p*PVC (Here, it is *p*PVC-3) showed reduced stretching vibration band corresponding to C-Cl bonds at 632 and 698 cm^{-1}, signposting Van der Waals interaction of ATBC with C-Cl bonds of PVC. However, the C-H stretching vibration bands of PVC still dominates and showed in the range 2880 – 3008 cm^{-1}. For *np*CuPc molecule, the corresponding unique Raman bands are noticed at 592, 676, 824, 949, 1032, 1101, 1138, 1140, 1338, 1449 and 1525 cm^{-1} [30]. Furthermore, the interaction of PVC with *np*CuPc in presence of ATBC in *np*CuPc-*p*PVC-3 gel was well noticed by the presence of corresponding bands for *np*CuPc, ATBC, and PVC.

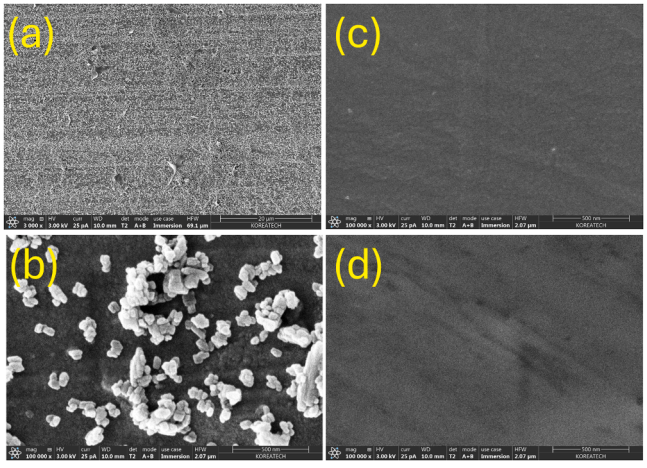


Fig. 1. (a-b) FESEM images of as-prepared *np*CuPc (low and high magnification, respectively), (c-d) surface and cross-sectional images of *np*CuPc-*p*PVC-3 gel.

The crystallographic structure of *b*CuPc, *np*CuPc, PVC (powder), and *np*CuPc-*p*PVC-3 gel were determined by XRD technique and presented in Fig. 2b. From the XRD spectra it is revealed that, the unique ($\bar{1}02$) crystal plane of CuPc was observed at 10.08°. In addition, 2θ = 23.68°, 26.32°, and 30.25° respectively corresponds to (112), ($\bar{3}13$), and ($\bar{4}13$) planes. The crystalline data were further confirmed by comparing with JCPDS cards no. 39–1881 [25], [31]. The XRD pattern of PVC exhibited its characteristic broad amorphous peaks at 2θ values around 17.5° and 24.5°. Further, *np*CuPc-*p*PVC-3 gel showed prominent dominating amorphous PVC peaks with slight downshift due to the interaction of PVC with ATBC and *np*CuPc. The thermal properties of as-prepared *b*CuPc, *np*CuPc, PVC (powder), and *np*CuPc-*p*PVC-3 were explored using TG analysis from ambient temperature to 700 °C and proffered in Fig. 2c. From TGA graph, *b*CuPc showed higher thermal stability, no degradation was noticed until 340 °C. However, 1.3 % weight loss was observed in case of *np*CuPc, demonstrating the nanostructured CuPc. Furthermore, PVC (powder) suffers in three degradation steps. The observed degradation for PVC (powder) ranges (100–210 °C, 270–350 °C, and 420–490 °C) are slightly higher than those traditionally reported for PVC. This can be attributed to the high molecular weight of the PVC used (Mw ≈ 233,000), controlled laboratory conditions such as heating rate and inert atmosphere, and the influence of adsorbed water/residual solvent molecules, which require additional energy for desorption before thermal decomposition begins. At around 100–210 °C was attributed to the adsorbed solvent molecules. The dehydrochlorination of PVC leading to polyenes was observed in the range 270–350 °C. The degradation of conjugated double bonds formed by dehydrochlorination of PVC was observed in the range 420–490 °C. The *np*CuPc-*p*PVC-3 gel showed slightly abridged thermal stability due to the plasticization effect of ATBC. The two major degradation steps were observed for *np*CuPc-*p*PVC-3 gel in the ranges 150–300 °C and 390–430 °C respectively for dehydrochlorination and polyenes degradation [32].

The electronic structure at the molecular-metal interface and the interaction of *np*CuPc in the PVC matrix was investigated by XPS analysis. The XPS spectra of as-fabricated *np*CuPc, *b*CuPc, *p*PVC-3, and *np*CuPc-*p*PVC-3 are presented and explained in Fig. S7-S10. respectively.

3.3. Dielectric, mechanical and electrical analysis

It is significant to measure the dielectric, mechanical, and electrical (in-plane/through-plane conductivity, leakage current) properties of *np*CuPc-*p*PVC gels, because these parameters eventually decide the haptic performances of the as-fabricated *np*CuPc-*p*PVC gel-based vibrotactile actuators. Dielectric performances of *np*CuPc-*p*PVC gels were measured and results were presented in Fig. 3a. It is evidently noticed that the dielectric constants of all the *np*CuPc-*p*PVC gels were found in the range of 8–12.5 at higher frequencies (100 Hz to 100,000 Hz). Dielectric properties declined steadily to 100 Hz and is directly proportional to the amount of *np*CuPc loading to *p*PVC. For *np*CuPc-*p*PVC-3 gel, the dielectric constant varied from 9.8 (at 100 Hz) to 9.0 (at 0.1 MHz).

The dielectric loss depicted in Fig. 3b. showed that all the gels suffer

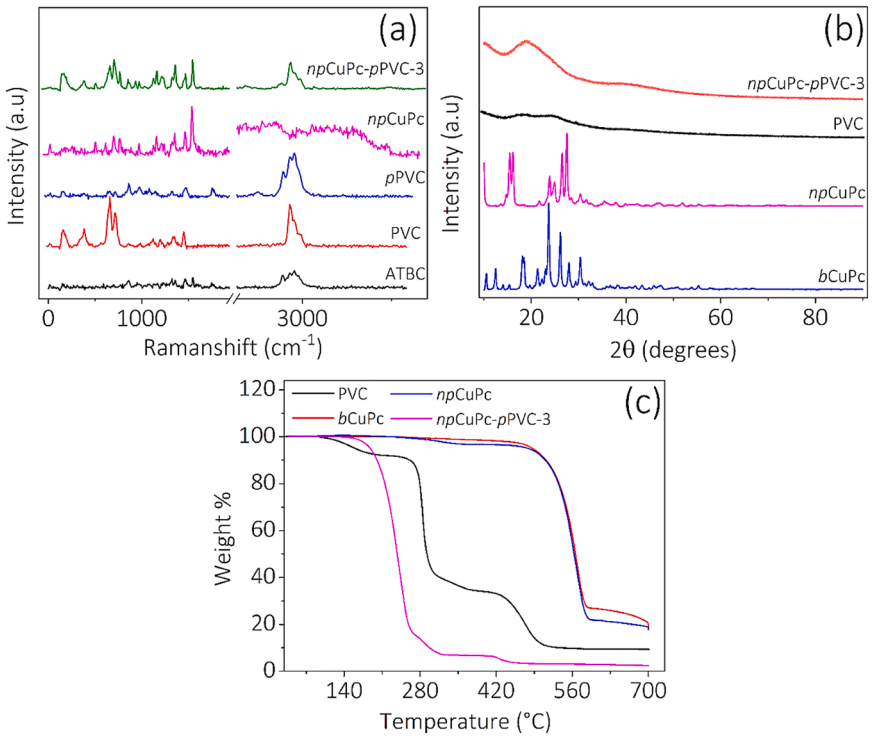


Fig. 2. (a) Raman, (b) XRD spectra, and (c) TG plots of as-prepared materials with PVC (powder), and ATBC.

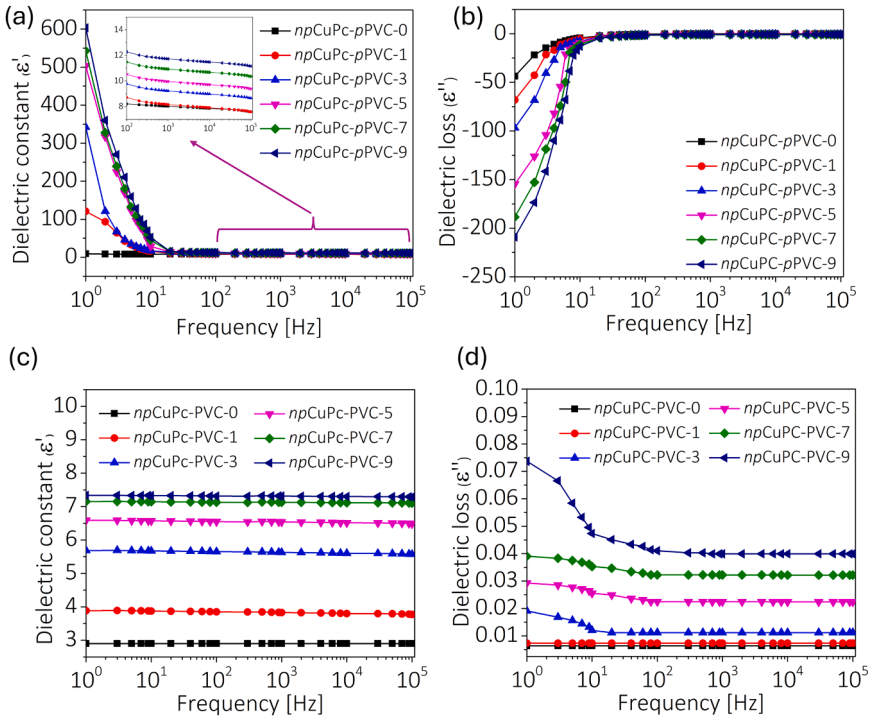


Fig. 3. (a, c) Variation of dielectric constant and (b, d) variation of dielectric loss for npCuPc–pPVC and npCuPc–PVC gels over the frequency range 1 Hz to 0.1 MHz. The inset in (a) highlights the dielectric constant variation in the range 10^2 Hz to 10^5 Hz.

abrupt fall in the values around −50.0 at lower frequency (1 Hz). The values further decreased with an increase of *np*CuPc content in the *p*PVC matrices.

The variation of dielectric constant and dielectric loss values with increasing *np*CuPc content in unplasticized PVC (without plasticizer, ATBC) were also investigated and presented in Fig. 3c. and Fig. 3d. The dielectric constant of unplasticized PVC with increased *np*CuPc content was steadily increased and it was reached the value 7.4 for *np*CuPc-PVC-9 in the frequency range 1 Hz to 0.1 MHz. The dielectric loss values for unplasticized PVC with increased *np*CuPc was well below 0.05 in the frequency range 100 Hz to 0.1 M Hz.

The negative dielectric loss observed at low frequencies is not

indicative of energy generation. It is generally considered an artifact caused by electrode polarization, interfacial effects, or phase lag between applied field and material response in heterogeneous systems. Such anomalies have been reported in polymer composites and arise from measurement limitations rather than physical energy gain.

Fig. 4a. portrays the mechanical properties of *np*CuPc-*p*PVC gels. The mechanical stiffness of the gels was directly proportional to the amount of *np*CuPc loading in *p*PVC matrix. In addition, all the gels were candidly strained to 250 %, which shows the mechanical flexibility and stretchability of as-prepared *np*CuPc-*p*PVC gels. The leakage current measurements [33] were performed for 10 mm × 10 mm flat gels with ~1 mm thickness, and the results were displayed in Fig. 4b. The maximum measured leakage current was ~1.75 μA for *np*CuPc-*p*PVC-1 gel. The leakage current values were exponentially declined to the minimum value of 0.52 μA for the maximum loading of *np*CuPc to *p*PVC (*np*CuPc-*p*PVC-9), suggesting the efficient utilization of electric power for the actuation.

AC impedance measurements were done in the frequency range between 100 kHz and 10 MHz to analyze the in-plane and through-plane surface resistance of *np*CuPc-*p*PVC gels using a two-probe technique with a PARSTAT potentiostat at a relative laboratory humidity of ~32 %. The results were displayed in Fig. 4c. The through-plane conductivity of the gels was initially escalated to 2.3×10^{-5} S/cm (for 0.3 wt% of *np*CuPc) from 1.2×10^{-5} S/cm (for 0.1 wt% of *np*CuPc). Furthermore, the through-plane conductivity was not altered much with additional loading of *np*CuPc to *p*PVC. This is due to the dielectric behavior and saturated distribution of *np*CuPc inside the PVC matrices under the influence of ATBC. Similar trend was noticed for the in-plane conductivity of the gels. For 0.1 wt% of *np*CuPc to *p*PVC, 0.09×10^{-3} S/cm was noticed initially and the values increased to the maximum of 2.1×10^{-2} S/cm (for 0.3 wt% of *np*CuPc) and steeply decreased afterwards to 2.2×10^{-3} S/cm with further increased content of *np*CuPc.

3.4. Actuator design, fabrication and acceleration studies

The design of the vibrotactile actuator and its fabrication process was previously developed from our research group - Interaction Laboratory [26,27,34]. In short, the structural apparatuses of the actuator were composed of three prime parts: (i) top component, (ii) dielectric layer (*np*CuPc-*p*PVC gel), and (iii) bottom component. The dimensions of the actuator were 2.5 cm (W) × 2.5 cm (L) × 0.05 cm (T). The wave-shaped *np*CuPc-*p*PVC gel was used as a dielectric interface and is sandwiched amid top and bottom component of the actuator. The gold electrode was used to cover the inner layers of top and bottom components to establish the fine electrical contact. The detailed design of the vibrotactile actuator was depicted in Fig. S11. The experimental conditions were optimized to find the best performing *np*CuPc-*p*PVC gel as soft and flexible vibrotactile actuator, accordingly by emplacing an experimental set up as shown in Fig. S12. The detailed design of the vibrotactile actuator was previously reported [26,27,34]. The experimental conditions were optimized to find the best performing *np*CuPc-*p*PVC gel as soft and flexible vibrotactile actuator, accordingly by emplacing an experimental set up [26,27,34]. In detail, a 100 g mass was affixed on the *np*CuPc-*p*PVC gel-based actuator. The experimental conditions were optimized and an input voltage of 1 kV and 160 Hz (resonant frequency) with sinusoidal wave was applied to determine the best performing *np*CuPc-*p*PVC gel. Predictably, *np*CuPc-*p*PVC-3 gel showed highest acceleration (0.88 g, where $g = 9.8\ ms^{-2}$) among the other investigated *np*CuPc-*p*PVC gels. The actuation results of *np*CuPc-*p*PVC-3 gel-based actuator was displayed in Fig. 5a. The robustness and durability of the *np*CuPc-*p*PVC-3 gel-based actuator was further operated for three incessant days. The actuation performances were minimally reduced (0.871 g) compared to its original value (0.88 g). This demonstrates the reliability of the *np*CuPc-*p*PVC-3 gel-based actuator (Fig. 5b.). The actuation performances of all the other *np*CuPc-*p*PVC gels were also carried out and shown in Fig. S13.

The variation of dielectric constant (*np*CuPc-*p*PVC gels and *np*CuPc-PVC thin films) at 100 Hz, Young's modulus and leakage current values accordingly to the weight % of *np*CuPc to *p*PVC were depicted in Fig. 6 (a-d) respectively. Fig. 6a shows a positive linear correlation between the dielectric constant and the weight percentage of *np*CuPc in the *p*PVC matrix. As the weight percentage of *np*CuPc increases, the dielectric constant increases steadily, indicating that the addition of *np*CuPc enhances the material's ability to store electrical energy. The variation of dielectric constant (*np*CuPc-*p*PVC gels and *np*CuPc-PVC thin films) at 100 Hz, Young's modulus and leakage current values accordingly to the weight % of *np*CuPc to *p*PVC were depicted in Fig. 6(a-d) respectively. Fig. 6a shows a positive linear correlation between the dielectric

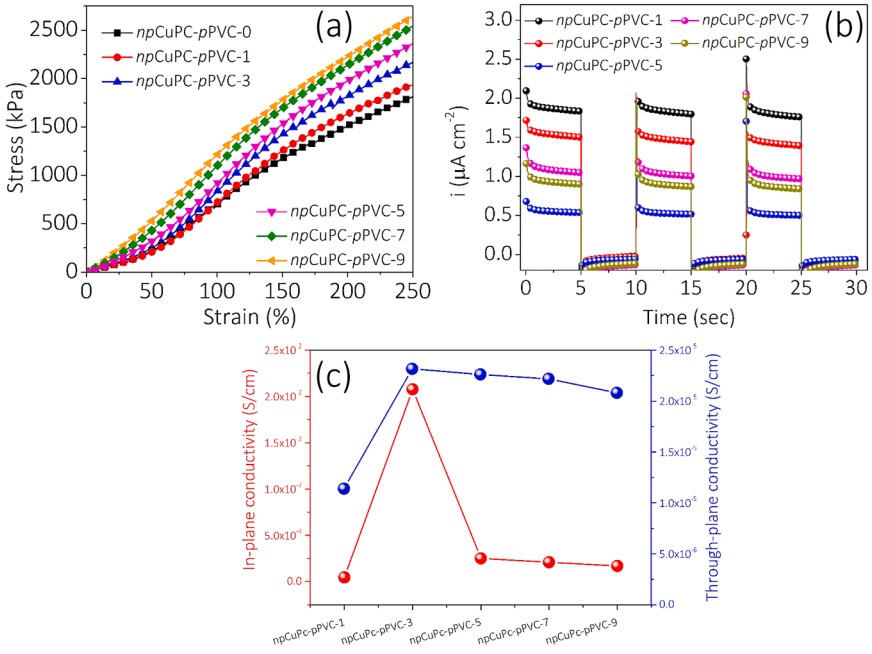


Fig. 4. (a) Stress–strain curves, (b) Leakage current plots (c) In-plane and through-plane conductivity of *np*CuPc-*p*PVC gels.

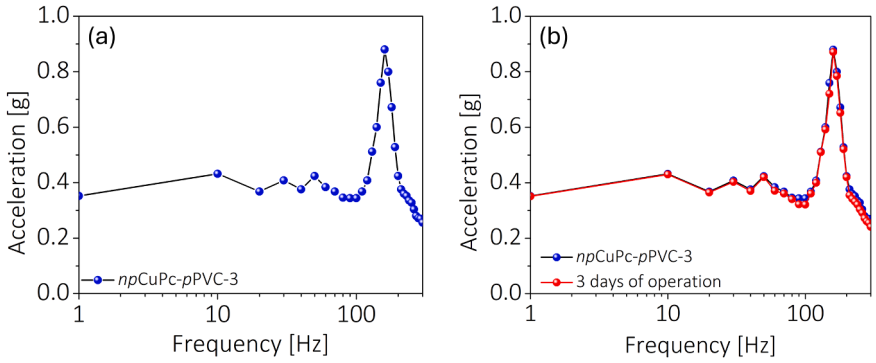


Fig. 5. (a) Acceleration performance of *np*CuPc-*p*PVC-3 gel, (b) Acceleration results of *np*CuPc-*p*PVC-3 gel under three days of continues operation.

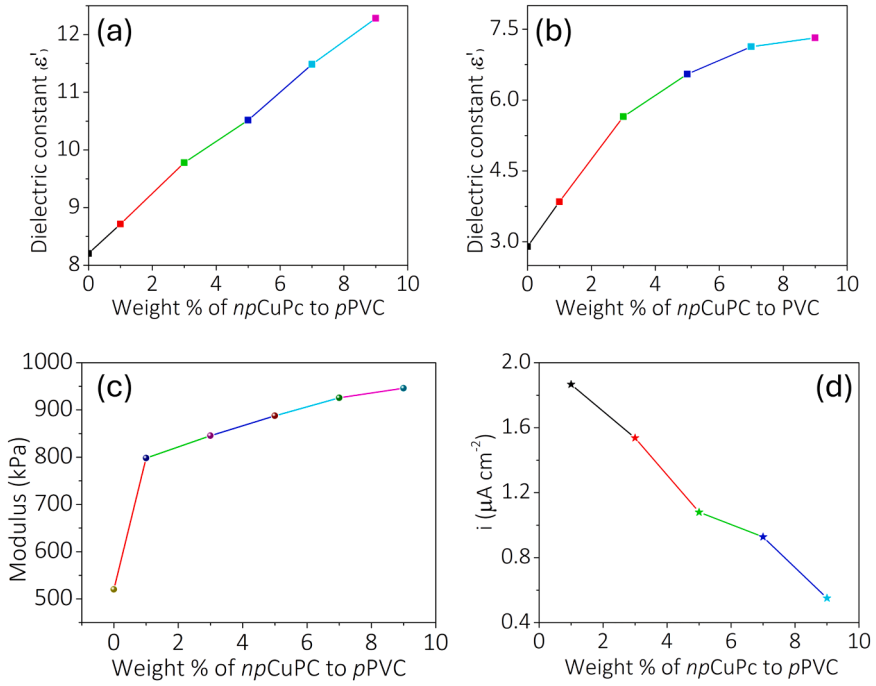


Fig. 6. (a-b) Variation of dielectric constant of *np*CuPc-*p*PVC gel and *np*CuPc-PVC thin films at 100 Hz, (c) variation of Young's modulus, (d) variation of leakage current, accordingly to the weight % of *np*CuPc to *p*PVC.

constant and the weight percentage of *np*CuPc in the *p*PVC matrix. As the weight percentage of *np*CuPc increases, the dielectric constant increases steadily, indicating that the addition of *np*CuPc enhances the material's ability to store electrical energy. Similar trend was noticed for weight percentage of *np*CuPc in the (unplasticized) PVC matrix. The initial drift is linear and not much increase in the dielectric constant for high weight percentages *np*CuPc (Fig. 6b). The Fig. 6c indicates an increasing modulus with the increasing concentration of *np*CuPc up to approximately 6–8 % by weight. Beyond this threshold, the modulus begins to level off or exhibit a slight decline, suggesting that the *np*CuPc contributes to enhancing the stiffness or rigidity of the *p*PVC composite at moderate concentrations, but further additions reach a saturation point, causing some degradation in the mechanical strength, potentially due to agglomeration and incompatibility at higher concentrations of *np*CuPc. Fig. 6d shows the leakage current (i) versus the weight percentage of *np*CuPc in *p*PVC. We noticed a negative trend as the *np*CuPc concentration increases, the leakage current decreases. This behavior suggests that *np*CuPc act as an insulator to reduce the material's conductivity. The decrease in the leakage current could be due to the disruption of conduction pathways in the high-*k* electret gel composites, possibly indicating a transition to a more dielectric behavior as the filler material (*np*CuPc) content increases. Collectively addition of dielectric filler, *np*CuPc into *p*PVC influences key material properties.

The detailed material (dielectric, mechanical, and electrical) properties of the fabricated gels are briefly outlined in Table 1. The acceleration data of the respective gels were briefly tabulated in Table 2.

To evaluate the versatility of the optimized actuator (*np*CuPc-*p*PVC-3), displacement (in μm) was measured as a function of applied voltage (Fig. 7). The displacement increased nearly linearly from 0.5 kV to 1.5 kV, followed by a slight saturation trend up to 2.0 kV. At the nominal operating point (1 kV), the actuator exhibited a displacement of approximately 28.3 μm, while the maximum displacement at 2.0 kV reached 48.6 μm. These results confirm the actuator's scalability across a broad voltage range and its stability under operational limits. To address the temperature stability in electret applications, thermal behaviour of the optimized actuator was measured using FLIR E6-XT (compact thermal imaging camera) under operational conditions. Continuous actuation tests showed a temperature variation of only 0.6 °C, which remained within the acceptable range for stable electret performance. The standard error was ±0.22 °C, based on repeated trials (n = 100). These results indicate minimal thermal drift and confirm that the material can operate reliably without significant heat accumulation

Table 1
Dielectric, mechanical, and electrical properties of *np*CuPc-*p*PVC gels.

Gel code	Dielectric constant at 1 Hz	Dielectric loss at 1 Hz	Young's modulus (kPa)	Maximal leakage current (μA)
np-CuPc-*p*PVC-0	7.55	-43.73	520.2	-
np-CuPc-*p*PVC-1	121.89	-68.44	798.1	1.88
np-CuPc-*p*PVC-3	342.54	-97.58	845.5	1.53
np-CuPc-*p*PVC-5	500.28	-155.05	887.6	1.08
np-CuPc-*p*PVC-7	540.24	-188.32	925.7	0.93
np-CuPc-*p*PVC-9	602.00	-210.33	946.1	0.56

Table 2
Acceleration performances of *np*CuPc-*p*PVC gels at the resonating frequency of 160 Hz.

Gel code	Maximum vibration acceleration (g), Note: g = 9.8 ms^{-2}
np-CuPc-*p*PVC-1	0.712
np-CuPc-*p*PVC-3	0.880
np-CuPc-*p*PVC-5	0.580
np-CuPc-*p*PVC-7	0.560
np-CuPc-*p*PVC-9	0.540

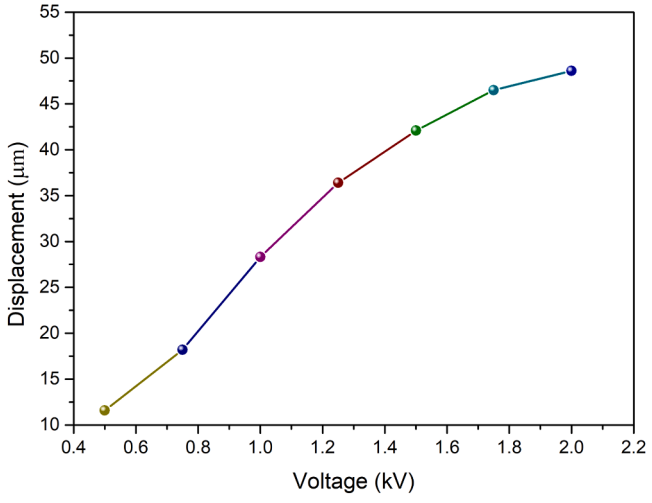


Fig. 7. Displacement of the optimized actuator (*np*CuPc-*p*PVC-3) as a function of applied voltage at a fixed frequency of 160 Hz.

from dielectric losses.

3.5. Instrumentation and characterization techniques

MALDI mass spectra was recorded on commercial time-of-flight mass spectrometers, A Kratos (Chestnut Ridge, NY) MALDI IV, operated with a nitrogen laser (337 nm) in the linear and positive ion mode. Surface and cross-sectional morphology and its Energy-dispersive X-ray analysis (EDXA) of *b*CuPc, *np*CuPc, and *np*CuPc-*p*PVC gels were investigated by Ultra-High-Resolution Field-Emission Scanning Electron Microscope (FESEM, FEI, & Nova NanoSEM450) instrument operating at 25 kV. Raman spectral (RM200) analysis was scanned in between 0 and 4000 cm^{-1} in presence of He and Ni laser beam. The crystalline and amorphous morphology of *b*CuPc, *np*CuPc, PVC, and *np*CuPc-*p*PVC gels were analyzed using RU-200B, X-ray diffractometer (XRD, Rigaku Rotaflex) with Cu-Ka radiation (λ = l.5406 nm). The distribution of elements and their valence states were examined via X-ray photoelectron spectroscopy (XPS, SPECSPHOIBOS-100 spectrometer, with Al anode (1486.7 eV) at 250 W); before study the nanocomposite surface was pre-cleaned by Ar^+ sputtering with low-energy beam at 3 keV, 5μA·cm^{-2} for 60 s. Thermal stability of as-prepared *b*CuPc, *np*CuPc, PVC, and *np*CuPc-*p*PVC gels were analyzed using thermogravimetric analyzer (Q500, TA instruments, DE, USA) in the range from 25 °C to 700 °C in a 50 mL/min N_2 gas flow at a heating rate of 10 °C/min.

For dielectric measurements, the flat gel samples were sandwiched between two gold plated electrodes and analysed by impedance analyzer, model HIOKI 3352–50 HiTESTER Version 2.3. The electrical contacts were checked to verify the ohmic connection. The measurements were carried out at room temperature in between the 1 Hz – 0.1 MHz.

The dielectric constant (ε') was calculated using an Eq. (1) and dielectric loss (tan δ) was calculated using an Eq. (2).

$$\varepsilon' = C_p \quad \times \quad d/\varepsilon_0 \times A \tag{1}$$

$$\tan\delta = \quad \varepsilon''/\varepsilon' \tag{2}$$

where 'd' is the thickness of the polymer film and '*A*' is the cross-section area, 'ε_o' is the permittivity of the free space, 'ε''' and 'ε'' is the permittivity (imaginary part) and permittivity (real part) of the material respectively. All these measurements were performed under dynamic vacuum.

The leakage current measurement was done using a potentiostat/galvanostat (Bio-logic Science Instruments, SP300) under an applied electric field of 800 V/mm at room temperature.

The method used to measure the in-plane (σ_{IP}) and through-plane conductivity (σ_{TP}) of npCuPc-pPVC gels are as follows:

Two equally spaced probes in contact with the measured gel material, and from the Nyquist plot, the resistance was extracted from the high-frequency intercept on the real axis and then the conductivity was calculated using the following Eqs. 3 and 4. The cell was operated at room temperature (at 30 % Relative humidity).

$$\sigma_{IP} = L/R \quad \times A \tag{3}$$

where σ_{IP} is the in-plane conductivity (S·cm^{-1}), L is the distance between the Pt electrodes (0.5 cm), R is the resistance (ohms), and A is the area of the gel (cm^2).

$$\sigma_{TP} = L/R \quad \times A \tag{4}$$

where σ_{TP} is the through-plane conductivity (S·cm^{-1}), L is the gel thickness, R is the bulk resistance of the gel, and A is the area of the gel (cm^2).

The experimental set-up for measuring the vibrational acceleration behavior is previously reported from our group [35]. In this experiment, the function generator (Protek 9305), a high voltage amplifier (Trek 10/40A-HS), an accelerometer (Bruel & Kjaer, Charge Accelerometer type 4393), a charge amplifier (Bruel & Kjaer, NEXUS Charge amplifier type 2692-A), and an oscilloscope (MSO/DPO 2000) was used. A square wave input voltage, with amplitude varied from 0 to 1 V with an interval of 0.1 mV, was amplified 1000 times by the high voltage amplifier. Then, the amplified input voltage was applied to the vibrotactile actuator. To measure the effective vibration acceleration of the as-fabricated *np*CuPc-*p*PVC gel-based actuators, a mass of 100 g was placed on the top layer of the actuator and measured the acceleration by projecting the accelerometer laser on the attached mass.

The developed electret actuator (*np*CuPc-*p*PVC-3) operates at 1.0 kV and achieves a high frequency of 160 Hz, delivering an acceleration of

0.88 g, which is competitive with other PVC gel systems. For instance, electroactive PVC gels reported by Park et al. [26] operate at the same voltage but at 100 Hz, producing 0.808 g acceleration. Similarly, silicon dioxide-PVC gels achieve 0.984 g at 100 Hz [26], while PANI–silicon dioxide-PVC gels reach 0.73 g at 130 Hz [27]. Ionic liquid-enhanced PVC gels exhibit large displacements in the range of 100–160 μm [36]. Compared to these systems, the developed electret actuator, *np*CuPc-*p*PVC-3 combines low-voltage operation, high-frequency capability, and competitive acceleration, making it highly suitable for compact vibrotactile applications.

4. Conclusions

We successfully synthesized *b*CuPc and transformed into *np*CuPc using hydrothermal route. As-prepared high dielectric constant organic semiconducting *np*CuPc was stoichiometrically loaded to the plasticized PVC (*p*PVC) for the fabrication of highly stretchable/flexible nanocomposite (*np*CuPc-*p*PVC) gels. As-prepared materials/nanocomposite gels were physicochemically characterized. The dielectric, mechanical, and electrical properties of these nanocomposite gels were skillfully exploited to fabricate *np*CuPc-*p*PVC gel-based vibrotactile actuators. The *np*CuPc-*p*PVC-3 (0.3 wt% *np*CuPc loading to *p*PVC) gel-based vibrotactile actuator exhibits upmost acceleration performance of 0.88 g at the resonant frequency of 160 Hz. Furthermore, the *np*CuPc-*p*PVC-3 gel-based actuators demonstrated its reliability and robustness with negligible performance loss even after 72 h operating conditions. Herein the investigation results demonstrated that, the *np*CuPc-*p*PVC gels are propitious dielectric interface materials for the fabrication of reliable smart vibrotactile actuators, which can disseminate diversified haptic sensation to the users.

CRediT authorship contribution statement

Ganesh Shimoga: Writing – review & editing, Writing – original draft, Validation, Supervision, Investigation, Conceptualization. **Sang-Youn Kim:** Supervision, Investigation, Funding acquisition. **Devendrachari Mruthyunjayachari:** Formal analysis. **Dong-Soo Choi:** Supervision, Funding acquisition. **Eun-jae Shin:** Formal analysis. **Seok-Han Lee:** Formal analysis.

Declaration of Competing Interest

The authors have no conflicts of interest to disclose.

Acknowledgements

We sincerely acknowledge the Cooperative Equipment Center at KOREATECH for FESEM, EDXA, RAMAN, XRD, XPS, and TG experimental assistance. The authors acknowledge KOREATECH for providing research opportunity and facilities. This research was supported by Basic Science Research Program through the National Research Foundation of Korea (NRF) funded by the Ministry of Education (RS-2023-00245538). This work was also supported by Institute of Information & communication Technology Planning & Evaluation (IITP) grant funded by the Korea government (MSIT) (No. RS-2024-00397310, Development of an AI Simulator for Creating Transparent Compounds that Can Be Altered for Tactile Sensation).

Appendix A. Supporting information

Supplementary data associated with this article can be found in the online version at doi:10.1016/j.sna.2025.117357.

Data availability

Data will be made available on request.

References

[1] B. Wang, W. Huang, L. Chi, M. Al-Hashimi, T.J. Marks, A. Facchetti, High- k gate dielectrics for emerging flexible and stretchable electronics, Chem. Rev. 118 (2018) 5690–5754, https://doi.org/10.1021/acs.chemrev.8b00045.
[2] S.H. Lee, S. Jeong, J. Moon, Nanoparticle-dispersed high-k organic–inorganic hybrid dielectrics for organic thin-film transistors, Org. Electron 10 (2009) 982–989, https://doi.org/10.1016/j.orgel.2009.05.009.
[3] G.I. Kim, J. Jung, W.K. Min, M.S. Kim, S. Jung, D.H. Choi, J. Chung, H.J. Kim, Mechanically durable organic/high- k inorganic hybrid gate dielectrics enabled by plasma-polymerization of PTFE for flexible electronics, ACS Appl. Mater. Interfaces 14 (2022) 28085–28096, https://doi.org/10.1021/acsami.2c04340.
[4] G. Shimoga, S.-Y. Kim, High-k polymer nanocomposite materials for technological applications, Appl. Sci. 10 (2020) 4249, https://doi.org/10.3390/app10124249.
[5] A. Valero, A. Mery, D. Gaboriau, M. Dietrich, M. Fox, J. Chretien, N. Pauc, P. Y. Jouan, P. Gentile, S. Sadki, Redefining high-k dielectric materials vision at nanoscale for energy storage: a new electrochemically active protection barrier, Electrochim. Acta 389 (2021) 138727, https://doi.org/10.1016/j.electacta.2021.138727.
[6] C. Deng, Y. Zhang, D. Yang, H. Zhang, M. Zhu, Recent progress on barium titanate-based ferroelectrics for sensor applications, Adv. Sens. Res. 3 (2024), https://doi.org/10.1002/adsr.202300168.
[7] L. Song, S. Glinsek, H. Ursic, S. Drnovsek, M. Sadl, B. Malic, E. Defay, Power-efficient piezoelectric haptic actuators with large deflection, Sens. Actuators A Phys. 356 (2023) 114346, https://doi.org/10.1016/j.sna.2023.114346.
[8] F. Ganet, M.-Q. Le, J.F. Capsal, J.F. Gérard, S. Pruvost, J. Duchet, S. Livi, P. Lermusiaux, A. Millon, P.-J. Cottinet, Haptic feedback using an all-organic electroactive polymer composite, Sens. Actuators B Chem. 220 (2015) 1120–1130, https://doi.org/10.1016/j.snb.2015.06.071.
[9] H.T. Tazwar, M.F. Antora, I. Nowroj, A.Bin Rashid, Conductive polymer composites in soft robotics, flexible sensors and energy storage: fabrication, applications and challenges, Biosens. Bioelectron. X (2025) 100597, https://doi.org/10.1016/j.biosx.2025.100597.
[10] D. Pyo, S. Ryu, K.-U. Kyung, S. Yun, D.-S. Kwon, High-pressure endurable flexible tactile actuator based on microstructured dielectric elastomer, Appl. Phys. Lett. 112 (2018), https://doi.org/10.1063/1.5016385.
[11] S.-C. Lin, W.-P. Shih, P.-Z. Chang, Microstructural dielectric elastomer actuator with uniaxial in-plane contraction, J. Intell. Mater. Syst. Struct. 24 (2013) 347–356, https://doi.org/10.1177/1045389X12451193.
[12] B. Wang, W. Huang, L. Chi, M. Al-Hashimi, T.J. Marks, A. Facchetti, High- k gate dielectrics for emerging flexible and stretchable electronics, Chem. Rev. 118 (2018) 5690–5754, https://doi.org/10.1021/acs.chemrev.8b00045.
[13] C.-P. Wong, W. Lin, L.-B. Zhu, H.-J. Jiang, R.-W. Zhang, Y. Li, K.-S. Moon, Nano materials for microelectronic and photonic packaging, Front. Optoelectron. China 3 (2010) 139–142, https://doi.org/10.1007/s12200-010-0009-9.
[14] P.N. Mohan, C. Thirmal, A. Joseph, B. Arun, K.S. Priya, P. Murugavel, K.C.J. Raju, Microwave, ferroelectric and electromechanical studies of free standing blended electroactive polymer films, Mater. Res. Bull. 181 (2025) 113105, https://doi.org/10.1016/j.materresbull.2024.113105.
[15] L.N. Ismail, S. Samsul, M.Z. Musa, S. Norsabrina, Fabrication of p-type organic field effect transistor using PMMA:TiO 2 as nanocomposite dielectric layer, IOP Conf. Ser. Mater. Sci. Eng. 340 (2018) 012005, https://doi.org/10.1088/1757-899X/340/1/012005.
[16] J.-W. Zha, M.-S. Zheng, B.-H. Fan, Z.-M. Dang, Polymer-based dielectrics with high permittivity for electric energy storage: a review, Nano Energy 89 (2021) 106438, https://doi.org/10.1016/j.nanoen.2021.106438.
[17] K. Liu, B. Ouyang, X. Guo, Y. Guo, Y. Liu, Advances in flexible organic field-effect transistors and their applications for flexible electronics, Npj Flex. Electron 6 (2022) 1, https://doi.org/10.1038/s41528-022-00133-3.
[18] B.J. Kim, E. Meng, Review of polymer MEMS micromachining, J. Micromech. Microeng. 26 (2016) 013001, https://doi.org/10.1088/0960-1317/26/1/013001.
[19] Bauer, Piezo-, pyro- and ferroelectrets: soft transducer materials for electromechanical energy conversion, IEEE Trans. Dielectr. Electr. Insul 13 (2006) 953–962, https://doi.org/10.1109/TDEI.2006.247819.
[20] R. Ramprasad, N. Shi, Polarizability of phthalocyanine based molecular systems: a first-principles electronic structure study, Appl. Phys. Lett. 88 (2006), https://doi.org/10.1063/1.2209197.
[21] N. Shi, R. Ramprasad, Dielectric properties of Cu-phthalocyanine systems from first principles, Appl. Phys. Lett. 89 (2006), https://doi.org/10.1063/1.2339037.
[22] X. Yang, Q. Wang, Y. Zhang, Z. Jiang, The microstructure and dielectric properties of modified poly(aryl ether ketone)/metallophthalocyanine composites, Polym. J. 44 (2012) 1042–1047, https://doi.org/10.1038/pj.2012.50.
[23] J. Wang, C. Wu, R. Liu, S. Li, Enhanced dielectric behavior in nanocomposites of polyurethane bonded with copper phthalocyanine oligomers, Polym. J. 46 (2014) 285–292, https://doi.org/10.1038/pj.2013.101.
[24] S. Fan, Y. Bin, R. Zhang, P. Zhang, D. Zhu, M. Matsuo, Dielectric Change of Copper Phthalocyanine and Polyurethane Foam with High Elasticity as a Function of Pressure Discussed in Terms of Conversion from Natural Mechanical Energy to Electric Energy, Macromolecules 47 (2014) 8281–8294, https://doi.org/10.1021/ma5014447.
[25] L. Tong, R. Wei, X. LiuNovel in-situ nanocomposites of phthalonitrile end-capped polyarylene ether nitrile/copper phthalocyanine, in: 2017: p. 020032. https://doi.org/10.1063/1.4971914..
[26] W.-H. Park, E.-J. Shin, S. Yun, S.-Y. Kim, An enhanced soft vibrotactile actuator based on ePVC gel with silicon dioxide nanoparticles, IEEE Trans. Haptics 11 (2018) 22–29, https://doi.org/10.1109/TOH.2018.2808176.

[27] G. Shimoga, E.-J. Shin, S.-Y. Kim, Flexible vibrotactile actuator based on soft PVC gel embedded polyaniline/silicon dioxide nanoparticles, IEEE Access 8 (2020) 122057–122064, https://doi.org/10.1109/ACCESS.2020.3006962.
[28] M.J. Giuliodori, H.L. Lujan, W.S. Briggs, G. Palani, S.E. DiCarlo, Hooke's law: applications of a recurring principle, Adv. Physiol. Educ. 33 (2009) 293–296, https://doi.org/10.1152/advan.00045.2009.
[29] X. Zhang, Y. Li, J.M. Hankett, Z. Chen, The molecular interfacial structure and plasticizer migration behavior of "green" plasticized poly(vinyl chloride), Phys. Chem. Chem. Phys. 17 (2015) 4472–4482, https://doi.org/10.1039/C4CP05287K.
[30] S. Kumar, N. Kaur, A.K. Sharma, A. Mahajan, R.K. Bedi, Improved Cl 2 sensing characteristics of reduced graphene oxide when decorated with copper phthalocyanine nanoflowers, RSC Adv. 7 (2017) 25229–25236, https://doi.org/10.1039/C7RA02212C.
[31] M. Samanta, P. Howli, U.K. Ghorai, M. Mukherjee, C. Bose, K.K. Chattopadhyay, Solution processed Copper Phthalocyanine nanowires: A promising supercapacitor anode material, Phys. E Low. Dimens. Syst. Nanostruct. 114 (2019) 113654, https://doi.org/10.1016/j.physe.2019.113654.
[32] J. Yu, L. Sun, C. Ma, Y. Qiao, H. Yao, Thermal degradation of PVC: A review, Waste Manag 48 (2016) 300–314, https://doi.org/10.1016/j.wasman.2015.11.041.
[33] H. Park, S. Oh, D. Kim, M. Kim, C. Lee, H. Joo, I. Woo, J.W. Bae, J. Lee, Plasticized PVC-gel single layer-based stretchable triboelectric nanogenerator for harvesting mechanical energy and tactile sensing, Adv. Sci. 9 (2022), https://doi.org/10.1002/advs.202201070.
[34] Y.H. Heo, S.H. Lee, I.K. Lee, S.-Y. Kim, Enhanced flexible vibrotactile actuator based on dielectric elastomer with propylene carbonate, Intell. Serv. Robot 17 (2024) 67–74, https://doi.org/10.1007/s11370-023-00503-4.
[35] W.-H. Park, J.W. Bae, E.-J. Shin, S.-Y. Kim, Development of a flexible and bendable vibrotactile actuator based on wave-shaped poly(vinyl chloride)/acetyl tributyl citrate gels for wearable electronic devices, Smart Mater. Struct. 25 (2016) 115020, https://doi.org/10.1088/0964-1726/25/11/115020.
[36] I. Ali, A. Latif, K. Hussain, F.K. Shehzad, A. Ali, R. Faisal, L. Xudong, O.A.T. Dias, Y. Weimin, L. Haoyi, Ionic liquids enhanced performance of PVC gels actuator, J. Appl. Polym. Sci. 138 (2021) e50710, https://doi.org/10.1002/app.50710.



Ganesh Shimoga earned his M.Sc. (Hons.) in Industrial Chemistry in 2004 and his Ph.D. in designing dielectric ionomers for technological applications in 2014, both from Kuvempu University, Karnataka, India. He began his career as a Research and Development Scientist at BIOCON, where he worked for three years. From 2015 to 2018, he served as Junior Research Staff at the Centrum polymerních systémů (CPS), Tomas Bata University, Czechia. He later became a Research Professor at the Interaction Laboratory led by Prof. Dr. S.-Y. Kim at Korea University of Technology and Education (KOREATECH). He is currently a Research Scientist at SINTEF Industry, Norway, in Polymer Particles and Surface Chemistry research group. He is passionate about developing dielectric materials/polymers, organic semiconducting materials, stretchable hydrogels, sensors and actuators, as well as drives innovation in designing new metal and molecular-based electrocatalysts for energy conservation and conversion devices (batteries and supercapacitors).



Eun-Jae Shin received the BS and MSE degrees from the Korea University of Technology and Education (KOREATECH), in 2014 and 2016, respectively. She is a doctoral course student inKOREATECH. Her research interest includes studying transparent and stretchable electroactive polymer and soft haptic actuators.



Seok-Han Lee received a B.S. (2019) degree in Computer Science Engineering from the Korea University of Technology and Education. He is currently a Master's and doctorate courses student of the Interdisciplinary Program in Creative Engineering from the Korea University of Technology and Education (KOREATECH). His current research interests include human-computer interaction, human-robot interaction, haptics, smart material, haptic sensor.



Mruthyunjayachari C. D. Mruthyunjayachari C. D. Received his B.Sc. (2007), M.Sc. (2009), and Ph.D. (2019) degrees in Industrial Chemistry from Kuvempu University, India. From 2009 to 2012, he worked as an Executive in the Quality Control Department at Biocon Pvt. Ltd. He then served as a Research Assistant (2015–2019) and subsequently as a Research Associate (2019–2021) in the Department of Chemistry at IISER Pune, India. He is currently a researcher in the Interaction Laboratory at Korea University of Technology and Education. His present research focuses on electrochemical energy storage applications, as well as the design and synthesis of advanced materials for cutting-edge technologies.



Dong-Soo Choi received his B.S. (2013), M.S. (2015), and Ph. D. (2020) degrees in Computer Science and Engineering from Korea University of Technology and Education (KOREATECH), Korea. He served as an Assistant Professor at Semyung University from 2020 to 2022, and subsequently as an Assistant Professor in the Department of Computer Engineering at Kumoh National Institute of Technology from 2022 to 2025. He is currently an Associate Professor in the same department at Kumoh National Institute of Technology, Korea. His research interests include immersive VR/AR, haptics, transparent pressure sensors, 3D touch sensors, vibrotactile actuators, and focus-tunable lenses.



Sang-Youn Kim received his B.S. degree from Korea University, South Korea, in 1994, and M. S. and Ph.D. degrees from the Department of Mechanical Engineering, Korea Advanced Institute of Science and Technology (KAIST) in 1996 and 2004, respectively. From 2004 to 2005, he was a researcher at the Human Welfare Robot System Research Center. In 2005, he was a research staff member at the Samsung Advanced Institute of Technology. He is currently a professor of computer science and engineering at the Korea University of Technology and Education. His current research interests include human-computer interaction, virtual reality, and haptics.